ACS OMEGA

http://pubs.acs.org/journal/acsodf

Article

Assessment of Anticorrosion Performance of Zinc-Rich Epoxy Coatings Added with Zinc Fibers for Corrosion Protection of Steel

Chunping Qi, Claus Erik Weinell, Kim Dam-Johansen, and Hao Wu*

Cite This: *ACS Omega* 2023, 8, 1912−1922

Read Online

ACCESS | Metrics & More | Article Recommendations | Supporting Information

ABSTRACT: The effect of adding 0.5 wt % zinc fibers on the anticorrosion performance of zinc-rich epoxy (ZRE) coatings with 85, 75, and 65 wt % of zinc dust was investigated. The salt spray testing, scanning electron microscopy, open circuit potential, and electrochemical impedance spectroscopy measurements were used to characterize the corrosion protection performance of coatings. The results indicate that the ZRE coating containing 85 wt % zinc dust showed superior cathodic protection, while the coating with 65 wt % zinc dust provided neither cathodic protection nor good barrier protection. No significant improvement in the anticorrosion performance was observed for both coatings with the addition of 0.5 wt % zinc fibers. In contrast, the ZRE coating containing 75 wt % zinc dust, which provided short-term cathodic protection followed by barrier protection, showed remarkably improved anticorrosion performance with the addition of zinc fibers.

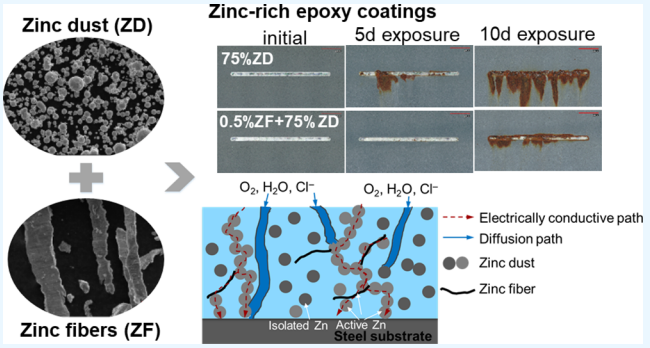

1. INTRODUCTION

Zinc-rich coatings, constituted by a high level of metallic zinc with either organic (such as epoxy) or inorganic (such as inorganic silicates) binders, have been one of the most popular heavy-duty coatings for the protection of steel surfaces against corrosion.[1] Nowadays zinc-rich epoxy (ZRE) coatings are increasingly popular because of their high tolerance to application and surface preparation.[2]

Zinc-rich coatings provide corrosion protection based on two primary mechanisms: cathodic protection from active zinc particles in the coating and subsequent barrier protection improved by the effective pore-filling with corrosion products in the coating.[3] Zinc content and zinc particle shape have a major influence on the cathodic protection of zinc-rich coatings.[4] The most common commercial zinc pigment is spherical shaped zinc dust, which makes only weak point contact with adjacent particles. To achieve a high cathodic protection performance, a content of zinc dust higher than 80 wt % is usually required to achieve good electrical contacts among the zinc particles in the coating film and between the zinc particles and steel substrate. However, only around one-third of the added zinc in a standard ZRE coating contributes to cathodic protection.[5] Moreover, such a high zinc content could cause problems such as high coating porosity, weak adhesion strength, poor coating mechanical properties (low flexibility and crack resistance), and in-can segmentation of zinc.[6]

Therefore, many efforts have been made to reduce zinc loading and/or improve the anticorrosive properties of zinc-rich coatings. Surface modification of zinc is a common way to reduce the particle electrochemical activity by forming a complex layer on its surface and thus prolongs the cathodic protection time of zinc-rich coatings.[7,8] The incorporation of lamellar pigments such as lamellar Al particles, micaceous iron oxide, and clay nanolayers has been reported to decrease the zinc consumption rate by hindering the electrolyte penetration and therefore extending the cathodic protection period.[9,10] In addition, phosphate-type pigments and hydrophobic additives such as TiO_2 nanoparticles and ionic liquids were incorporated to improve the inhibitive effect of zinc-rich coatings.[11−13] The electrical connectivity in zinc-rich coatings and hence the utilization efficiency of zinc particles can be improved by adding electrically conductive materials. Metallic nanoparticles such as Zn and Al nanoparticles,[14,15] conductive polymers/composites such as polypyrrole and polyaniline,[6,16−18] conductive pigments such as diiron phosphide (Fe_2P)[19] and stainless-steel flakes,[20] and many carbon-based additives such as biochar,[21] carbon nanotubes,[22,23] and graphene[1,24,25] are reported to effectively improve the film conductivity, leading to a better cathodic protective activity.

By far, several reinforcement fibers, which are commonly used as fillers to improve the mechanical properties of matrix

Received: June 15, 2022
Accepted: December 22, 2022
Published: January 5, 2023

https://doi.org/10.1021/acsomega.2c03738
ACS Omega 2023, 8, 1912−1922

like concrete, have been introduced into zinc-rich coatings. The incorporation of nonconductive fibers such as quartz fiber did not improve the coating performance.[26] However, conductive fibers such as carbon, graphite, and silicon nitride fibers were reported to enhance the coating performance remarkably because they increased the electrical connectivity and improved the utilization efficiency of zinc particles in the coating film. Also, the fibers hinder Cl^- ion penetration into the coating/steel interface.[27,28] Therefore, the incorporation of conductive reinforcing fibers into zinc-rich coatings seems to be able to lower the pigment content without affecting significantly the anticorrosion performance.

In this work, zinc fibers were used as electrical additives in the ZRE coatings. Zinc fibers, as with other conductive fibers, are expected to both improve the coating mechanical properties, and connect more zinc particles into electrically conductive paths, achieving the electronic percolation threshold at a reduced zinc content. In addition, the zinc fibers themselves also provide galvanic protection to the steel substrate. However, no research has been reported about the employment of zinc fibers in the ZRE coatings. In this work, a fixed amount of zinc fibers was added to the ZRE coatings containing various levels of zinc dust, and the coating anticorrosion performance was studied by salt spray and electrochemical tests with the aid of characterization by scanning electron microscopy (SEM) and energy dispersive spectroscopy (EDS).

2. EXPERIMENTAL SECTION

2.1. Preparation and Application of Coatings. Zinc dust (EverZinc Norway AS) used in this study consists of primarily spherical particles, and the diameter is 13 μm. Zinc fibers, specified with a width of 31 μm and length of 2.6 mm, were purchased from Stanford Advanced Materials. Zinc fibers were sieved using a 45 μm sieve to get finer fibers for the coating production. Figure S1 (in Supporting Information) depicts the particle morphology and size distribution of zinc dust and zinc fibers. All coatings were prepared based on a two-component epoxy system. The base part was prepared by mixing the zinc dust (and zinc fibers) together with bisphenol A epoxy resin (Hexion B.V.), solvent, antisettling agent, dispersant, and other ingredients using an ultrasonic mixer. The curing agent was a blend of accelerator, solvents, and formulated polyamide adduct. In the case of zinc fiber-added coatings, a fixed content (0.5 wt %) of zinc fibers was added to the coatings with different contents of zinc dust (65, 75, and 85 wt %). Such a small amount of zinc fibers were found to be well dispersed and distributed in the coating system without application problem in the preliminary tests. The coatings are denoted by the content (by weight) of zinc fiber and zinc dust, respectively. Table 1 lists the main compositions of the as-prepared coatings.

The as-prepared coatings were applied on a steel substrate with dimensions of 150 × 75 × 3 mm^3 using a 150 μm gap applicator. The steel substrate is hot-rolled S235 JR steel with medium roughness (Sa 2 1/2, Rz = 60−84 μm) purchased from Kent Bøge (Blacksmith, Kent Boege, DK-3650 Oelstykke). The steel surface has been pretreated by the supplier by a sequence of procedures according to the standard ISO 8501-1 involving degreasing, sandblasting, and de-dusting. All panels were used as received after dust removal by compressed air. The coated specimens were kept under laboratory conditions for one week prior to test. The dry film thickness was 80 ± 10 μm measured by an Elcometer gauge.

Table 1. Main Compositions of the Coatings

sample	zinc dust (wt %)	zinc fiber (wt %)	binder (wt %)	pigment volume concentration (%)
85ZRE	85	0	15	47.6
0.5ZF-85ZRE	85	0.5	14.5	48.6
75ZRE	75	0	25	32.7
0.5ZF-75ZRE	75	0.5	24.5	33.3
65ZRE	65	0	35	23.0
0.5ZF-65ZRE	65	0.5	34.5	23.4

2.2. Salt Spray Test. The accelerated corrosion test based on ISO 9227[29] was carried out in a neutral salt spray test chamber (exposure to a constant spray of 5 wt % NaCl aqueous solution under 35 °C). Experiments were performed in triplicate to ensure the reproducibility. After 90 days of salt spray test, the scribe creep was evaluated. After removing the loose coating around the scribe with a blade, the width of visible underfilm corrosion was measured at nine points according to ISO 12944-9.

2.3. Characterization. The crystal phases of coating films after the salt spray test was analyzed using a Huber G670 powder diffractometer (Rimsting, Germany) with Cu Kα1 radiation. Prisma E SEM (Thermo Fisher Scientific, USA) equipped with EDS was employed to examine the morphology and elemental composition of samples at an acceleration voltage of 20 keV. The subsurface defects of coated samples were detected by a nondestructive technique using scanning acoustic microscopy (SAM) with a PVA TePla SAM 301 HD^2 system at a frequency of 125 MHz.

2.4. Electrochemical Tests. Electrochemical analyses of coatings, including open circuit potential (OCP) and electrochemical impedance spectroscopy (EIS), were conducted on an electrochemical workstation (Reference 600+ Potentiostat, Gamry) using a three-electrode system. A graphite rod, a saturated calomel electrode (SCE), and the coated specimens with a test area of 10 cm^2 were the counter electrode, reference electrode, and working electrode, respectively. EIS was then measured in 3.5 wt % NaCl solution at room temperature. The measurements were performed at OCP with a frequency range of 10^5−10^{-2} Hz using a sinusoidal amplitude of 10 mV. The tests were performed in duplicate to ensure the data repeatability. The ZsimpWin software was used to analyze the obtained EIS data.

3. RESULTS AND DISCUSSION

3.1. Salt Spray Test. Figure 1 shows the visual observation of ZRE coatings with and without zinc fibers after the salt spray test. By looking at the samples without the addition of zinc fibers, red rust was observed at the scribed areas of both 75ZRE and 65ZRE coatings after one day exposure. In contrast, the 85ZRE coating showed superior cathodic protection and no red rust was formed at scribed areas until 25 days exposure. The amount of red rust decreased with increasing zinc content. The results demonstrated that an effective cathodic protection was afforded to the steel substrate by the coating with a high zinc content of 85 wt %.

The effect of adding 0.5 wt % zinc fibers on the coating performance was highly dependent on the content of zinc dust in the coatings. For the 85ZRE and 65ZRE coatings, no remarkably improved anticorrosion performance was observed

https://doi.org/10.1021/acsomega.2c03738
ACS Omega 2023, 8, 1912−1922

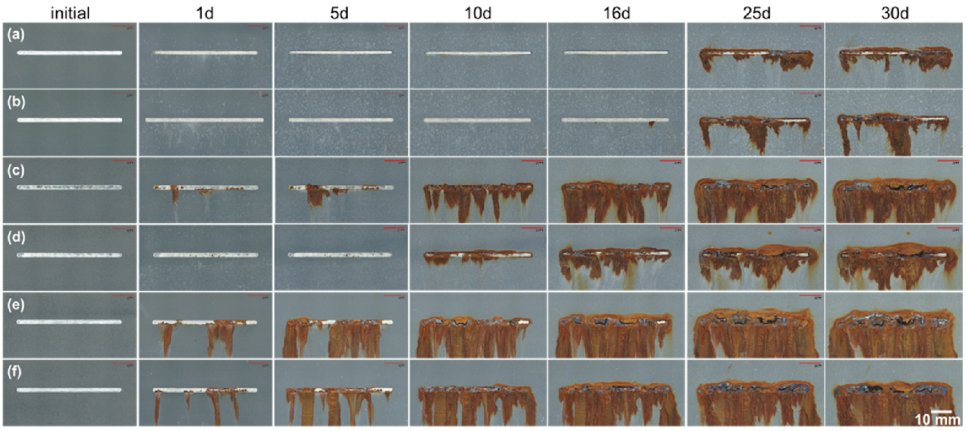

Figure 1. Photographs of ZRE coatings with and without adding zinc fibers during the salt spray test. (a) 85ZRE; (b) 0.5ZF-85ZRE; (c) 75ZRE; (d) 0.5ZF-75ZRE; (e) 65ZRE; (f) 0.5ZF-65ZRE.

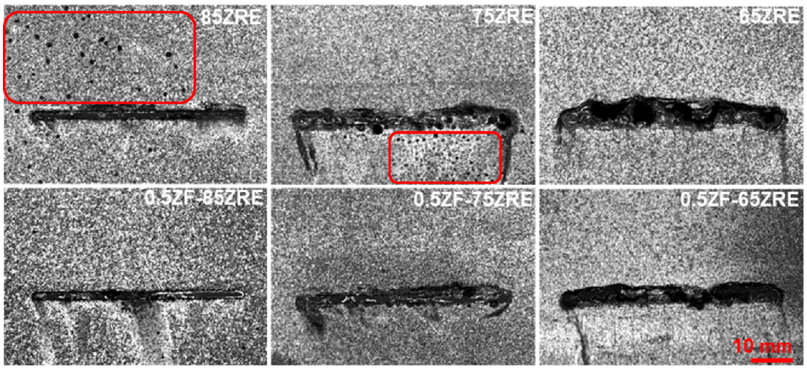

Figure 2. SAM images of ZRE coatings with and without adding zinc fibers after 30 days salt spray test (black spots are blisters and marked by the red boxes).

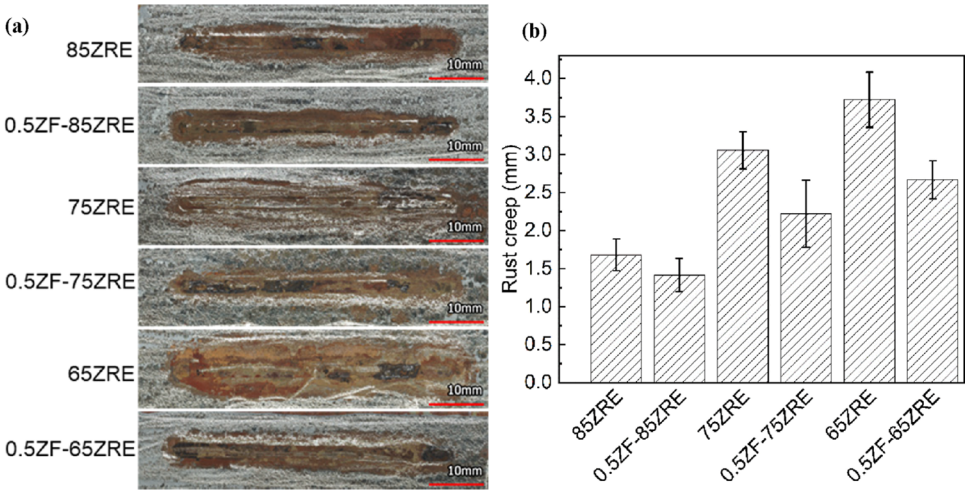

Figure 3. (a) Photograph of the surface after removing paint and (b) average scribe creep of coatings after 90 days salt spray test.

with the addition of zinc fibers. This is because the cathodic protection of ZRE coatings depends on an electronic charge percolation threshold, i.e., the lowest zinc content at which long range electrical conductivity becomes possible as a result of particle−particle contact. In this study, the zinc dust content of 85 wt % was more than adequate to achieve a good cathodic protection, and the addition of zinc fibers may even increase the coating porosity resulting in a poorer barrier property, whereas the zinc dust content of 65 wt % was far below the threshold to achieve sufficient electrical conductivity for cathodic protection even with the addition of 0.5 wt % zinc fibers. In contrast, a zinc dust content of 75 wt % was close to the threshold, and the addition of zinc fibers significantly improved the cathodic protection of the 75ZRE coating and therefore, no red rust was observed until 10 days exposure. The replicate test (Figure S2 in Supporting Information) shows similar results, which further support that the addition of 0.5

https://doi.org/10.1021/acsomega.2c03738
ACS Omega 2023, 8, 1912−1922

wt % zinc fibers enhanced the anticorrosion performance of the coating containing 75 wt % zinc dust.

After 30 days exposure, a few visible blisters were found on the surface of coatings containing 85 and 75 wt % zinc dust, and it is shown in Figure 2 by SAM images where the blackspots are visible blisters. In contrast, the addition of 0.5 wt % zinc fibers increased the blister resistance, and blisters were not observed on the surface of fiber containing coatings.

The result of average red rust creep at scribes is shown in Figure 3. It is clearly seen that the coatings exhibited less rust creep with increasing zinc content, indicating a better long-term corrosion protection performance. The addition of zinc fibers could further increase the rust creep resistance, and this effect was more pronounced for the coating with lower zinc dust contents (65 and 75 wt %).

3.2. X-ray Diffraction Characterization. To identify the composition of corrosion products, after 90 days salt spray test, coating films in the intact area, which were far from the scribe and no red rust was observed, were scrapped from steel panels and ground to fine powder for X-ray diffraction (XRD) characterization. As seen in Figure 4, the XRD analysis showed similar spectra for all coatings dominated by metallic Zn, which indicates that a large amount of zinc remained unconsumed. In addition, peaks associated with zinc corrosion products including $Zn_5(OH)_8Cl_2{\cdot}H_2O$, ZnO, and $Zn_5(CO_3)_2(OH)_6$ were observed, which agrees well with the zinc corrosion products reported in other studies.[30,31] Further, the relative intensity of peaks corresponding to ZnO (2θ = 32°, 47°, 57°, 63°, and 68°) became stronger with decreasing zinc content. The slightly soluble ZnO has been reported to provide worse long-term barrier protection than insoluble corrosion products $Zn_5(CO_3)_2(OH)_6$ and $Zn_5(OH)_8Cl_2{\cdot}H_2O$.[32]

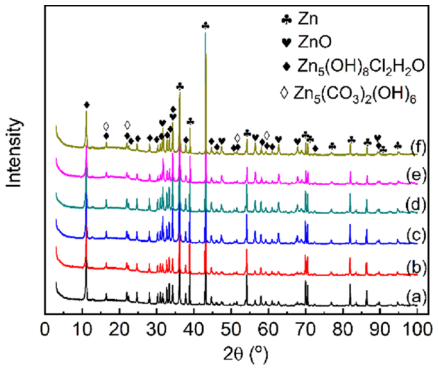

Figure 4. XRD spectra of different coatings after 90 days salt spray test. (a) 85ZRE; (b) 0.5ZF-85ZRE; (c) 75ZRE; (d) 0.5ZF-75ZRE; (e) 65ZRE; (f) 0.5ZF-65ZRE.

3.3. SEM−EDS Characterization. The corrosion protection of coatings was further studied by the aid of SEM−EDS analysis. All SEM-characterizations were performed in duplicate, and the results shown are representative. Figure 5 depicts the cross-section and surface SEM images of 85ZRE and 0.5ZF-85ZRE coatings before and after exposure. As seen in Figure 5a, before exposure, spherical zinc particles were distributed uniformly in the coating and in good electrical contact with themselves and with a steel substrate. With the addition of 0.5 wt % zinc fiber, very few long fibers can be observed because of its very low content (Figure 5d). After 30 days exposure, some zinc particles inside the coating were partially corroded forming nonconductive corrosion products on the particle surface. Additionally, a thick corrosion products layer was accumulated on the top surface of the two coatings. Likewise, the surface mircograph (Figure 5c) shows that the coating surface was completely covered by a large amount of zinc oxidation products, resulting in a spongy surface morphology. These observations confirm that efficient cathodic protection was afforded to the steel substrate by active zinc paticles in the coatings with 85 wt % zinc dust, while no corrosion of underlying steel substarte was observed. Surface and cross-section SEM images showed a similar morphology for the coatings in spite of the addition of 0.5 wt % zinc fibers.

Figure 6 displays the cross-section and surface micrographs of 75ZRE and 0.5ZF-75ZRE coatings before and after exposure. Compared to the coatings with 85 wt % zinc dust,

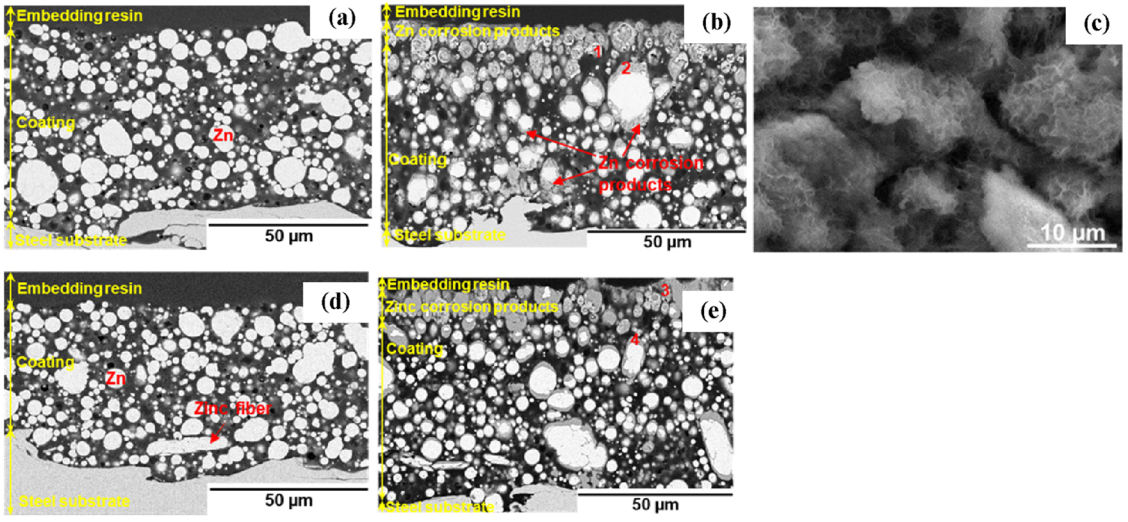

Figure 5. Cross-section and surface micrographs of 85ZRE and 0.5ZF-85ZRE coatings before and after 30 days exposure to salt spray. Cross-section of 85ZRE coating (a) before and (b) after exposure, (c) surface-view of 85ZRE coating after exposure, cross-section of 0.5ZF-85ZRE coating (d) before and (e) after exposure. (Cross-section and surface SEM micrographs in Figure 5−7 were obtained with a backscattered electron detector and secondary electron detector, respectively).

https://doi.org/10.1021/acsomega.2c03738
ACS Omega 2023, 8, 1912−1922

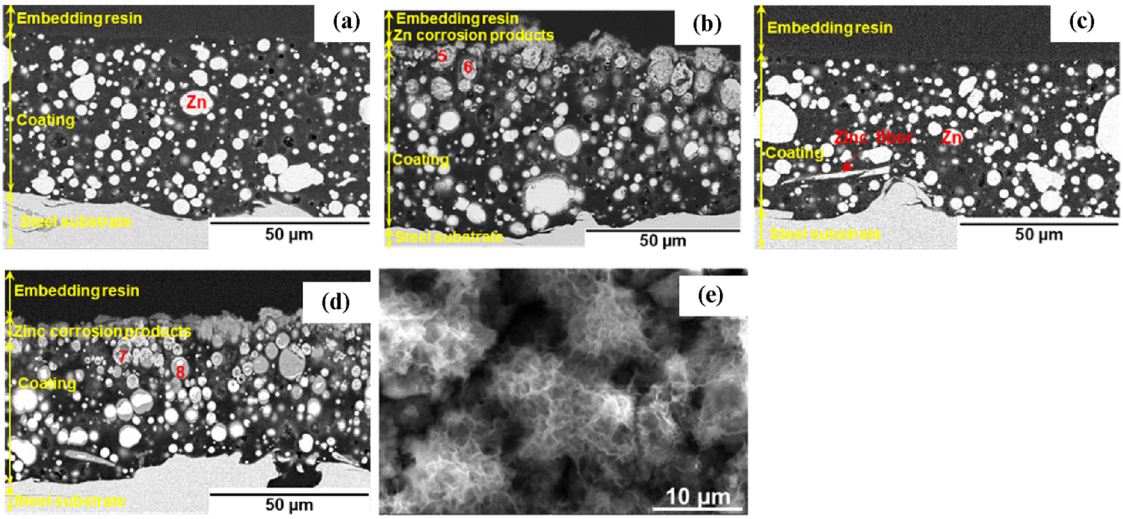

Figure 6. Cross-section and surface micrographs for 75ZRE and 0.5ZF-75ZRE coatings before and after 30 days exposure to salt spray. Cross-section of 75ZRE coating (a) before and (b) after exposure, 0.5ZF-75ZRE coating (c) before and (d) after exposure, and (e) surface-view of 0.5ZF-75ZRE coating after exposure.

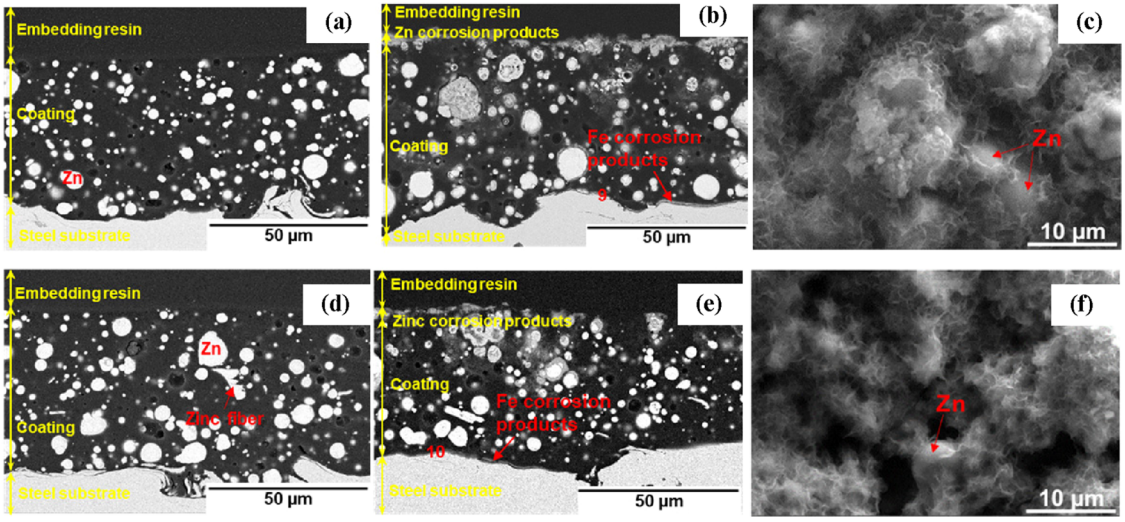

Figure 7. Cross-section and surface micrographs for 65ZRE and 0.5ZF-65ZRE coatings before and after 30 days exposure to salt spray. Cross-section of 65ZRE coating (a) before and (b) after exposure, (c) surface-view of 65ZRE coating after exposure, cross-section of 0.5ZF-65ZRE coating (d) before and (e) after exposure, and (f) surface-view of 0.5ZF-65ZRE coating after exposure.

an incorporation of fewer zinc particles results in less electrically conductive paths. Therefore, a thinner zinc corrosion product layer was formed on the top surface of the 75ZRE coating. In contrast, a slightly thicker zinc corrosion product layer was formed on the top coating surface with the addition of 0.5 wt % zinc fibers (when comparing Figure 6b,d) because of an increased electrical conductivity. This could result in a slightly higher coating resistance (R_c) during the late stage of exposure, which will be discussed in Section 3.4.2. Additionally, similar to the coatings with 85 wt % zinc dust, the spongy surface morphology of the 0.5ZF-75ZRE coating (Figure 6e) shows that the coating surface was covered by a large quantity of zinc corrosion products, forming a barrier layer at the coating/electrolyte interface.

Figure 7 shows the cross-section and surface micrographs for 65ZRE and 0.5ZF-65ZRE coatings. The cross-section images show that zinc particles in both coatings (Figure 7a,d) were mostly isolated by the epoxy resin, which cannot provide cathodic protection. Only a small amount of zinc corrosion products were observed after exposure, forming a very thin barrier layer which cannot fully cover the coating surface. As shown in Figure 7c, the morphology of the 65ZRE coating surface shows that some zinc particles remained in a spherical shape embeddng in the epoxy matrix, even with the addition of 0.5 wt % zinc fibers (Figure 7f). This implies that zinc particles were insufficient to afford effective cathodic protection even with the addition of 0.5 wt % zinc fibers. Further, precipitates were found at the coating/steel interface of panels coated with 65ZRE (Figure 7b) and 0.5ZF-65ZRE coatings (Figure 7e). Table 2 presents the elemental composition in different regions of coatings, while the corresponding element maps are shown in Figure S3 in Supporting Information. As shown in Table 2, the precipitates consisted of mainly zinc, iron, oxygen, and carbon, which indicates that the underlying steel corrosion was ongoing in both coatings. These observations show that coatings with 65 wt % zinc dust provide poor protection to the steel substrate. This will be discussed later in Section 3.4.2.

https://doi.org/10.1021/acsomega.2c03738
ACS Omega 2023, 8, 1912−1922

Table 2. Elemental Composition of Coatings after 30 Days Exposure Obtained from EDS Analysis (Unit: wt %[a])

sample	region	Zn	O	Cl	C	Fe
85ZRE	1	79.2	15.3	0.8	4.7	
	2	66.1	14.2	15.2	4.6	
0.5ZF-85ZRE	3	82.1	11.0	1.9	4.7	0.4
	4	68.1	12.0	15.0	4.7	0.3
75ZRE	5	80.2	11.4	1.0	6.7	0.3
	6	65.8	13.6	15.6	4.7	0.3
0.5ZF-75ZRE	7	81.6	11.5	0.7	5.3	0.9
	8	65.7	13.7	14.7	5.5	0.5
65ZRE	9	20.8	21.8	1.7	23.5	31.0
0.5ZF-65ZRE	10	11.1	21.8	0.7	18.7	47.7

[a]Elements with a content of <1.0 wt % are not shown in the table.

However, the presence of iron in EDS analysis could be also due to the influence of steel substrate proximity.

The SEM images and EDS results of all coatings show similar attack mechanisms of zinc particles and similar corrosion products within the coating. The zinc particles in the coating tend to be attacked uniformly forming corrosion products on the zinc particles' surface. The EDS results in regions 2, 4, 6, and 8 indicate the formation of chloride-based zinc complexes (possibly simonkolleite according to the XRD result) from the uniform dissolution of zinc.[30] In contrast, some zinc particles on the top surface show the formation of internal cavities, which results from the localized attack at certain points of the zinc surface. The regions 1, 3, 5, and 7 contain mainly zinc and oxygen, indicating the formation of zinc oxides/hydroxides because of the localized attack on the zinc particles.

3.4. Electrochemical Characterization of Coatings.

3.4.1. OCP Measurements. The cathodic protection capability and duration of coatings were analyzed by the OCP measurement. The corrosion potential of bare steel and zinc in seawater is reported to be approximately −0.65 and −1.05 V/SCE, respectively.[33] The threshold of cathodic protection for iron is an OCP lower than −0.86 V/SCE.[34,35] Figure 8 shows the OCP evolution over immersion time. All coatings exhibited a quick drop of the potential during the first 4 days induced by the electrolyte penetration and activation of zinc particles, which increases the active areas of zinc and leads to a better electrical connectivity.[34] When the zinc particles were mostly activated by the electrolyte, the potential reached a minimum value, and afterward it shifted to a more positive value gradually due to the formation of nonconductive corrosion products.

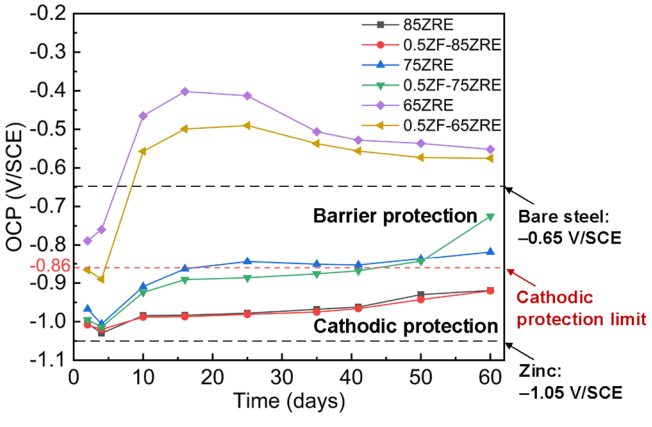

Figure 8. Variations of OCP for different coatings immersed in 3.5 wt % NaCl solution during 60 days.

From Figure 8, the addition of zinc fibers generally improves the electrical conductivity to a certain extent, resulting in more negative OCP values. The influence was decreased with incremental zinc content. The OCP values for the ZRE coatings with 65 wt % zinc dust (65ZRE and 0.5ZF-65ZRE coatings) were far more positive than −0.86 V/SCE, indicating the absence of effective cathodic protection. Although the addition of 0.5 wt % zinc fibers improved the electrical conductivity resulting in more negative OCP, it could not compensate the reduction of film conductivity caused by such a low zinc content. When the zinc dust content increased to 75 wt %, the presence of cathodic protection afforded by the 75ZRE coating during the first 16 days of immersion was confirmed by the low OCP values located in the cathodic protection region. Subsequently, the OCP of the 75ZRE coating shifted slightly to a more positive value than the cathodic protection limit and kept increasing gradually. With the addition of zinc fibers, the OCP values for the 0.5ZF-75ZRE coating were slightly more negative than those of the 75ZRE coating, and the values lie below the cathodic protection region within 41 days immersion. The results indicate that compared to the 75ZRE coating, the addition of zinc fibers created more electrically conductive paths to connect zinc particles with the steel substrate, resulting in a prolonged cathodic protection time. In contrast, the ZRE coatings containing 85 wt % zinc dust (85ZRE and 0.5ZF-85ZRE coatings) exhibited very similar OCP values below the cathodic protection limit during the entire test period. The result is replicable as indicated by the replicate measurements (Figure S4 in Supporting Information), and it is in consistence with the result of the salt spray test.

3.4.2. EIS Measurements. The barrier property of coatings and the corrosion processes were studied by EIS. The Bode plots of different coatings and $|Z|_{f=0.01\text{Hz}}$ values obtained from Bode plots are shown in Figures 9 and 10, respectively. The impedance modulus at low frequency (such as $|Z|_{f=0.01\text{Hz}}$) is a common parameter used for the qualitative evaluation of the barrier property of organic coatings. A higher $|Z|_{f=0.01\text{Hz}}$ value generally indicates better anticorrosion performance, and the coating degrades faster if the $|Z|_{f=0.01\text{Hz}}$ value drops more quickly.[36] It is clearly seen that the effect of zinc fibers on the impedance values was more pronounced at low zinc dust contents (65 and 75 wt %) when weak barrier protection was provided; with the addition of zinc fibers, the $|Z|_{f=0.01\text{Hz}}$ values of coatings decreased, because the addition of a small amount of zinc fibers to the coating was insufficient to block the microholes within the coating and may even increase the coating porosity because of their large particle size and thus reduce their barrier property. The coatings containing 85 wt % zinc dust exhibited an efficient cathodic protection with low impedance values. For the 85ZRE coating, the impedance values exhibited a plateau at approximately 15,000 Ω·cm^2 during the entire test period. With the addition of zinc fibers, the coating exhibited similar variation of Bode-impedance values and showed a slightly higher impedance value (approximately 18,000 Ω·cm^2) after 10 days of immersion. In contrast, a quick drop from 1,123,000 Ω·cm^2 (2d) to 564,000 Ω·cm^2 (10d) at the beginning and then a slow decrease to 192,100 Ω·cm^2 (60d) was observed for the impedance values of the 75ZRE coating, while the impedance

https://doi.org/10.1021/acsomega.2c03738
ACS Omega 2023, 8, 1912−1922

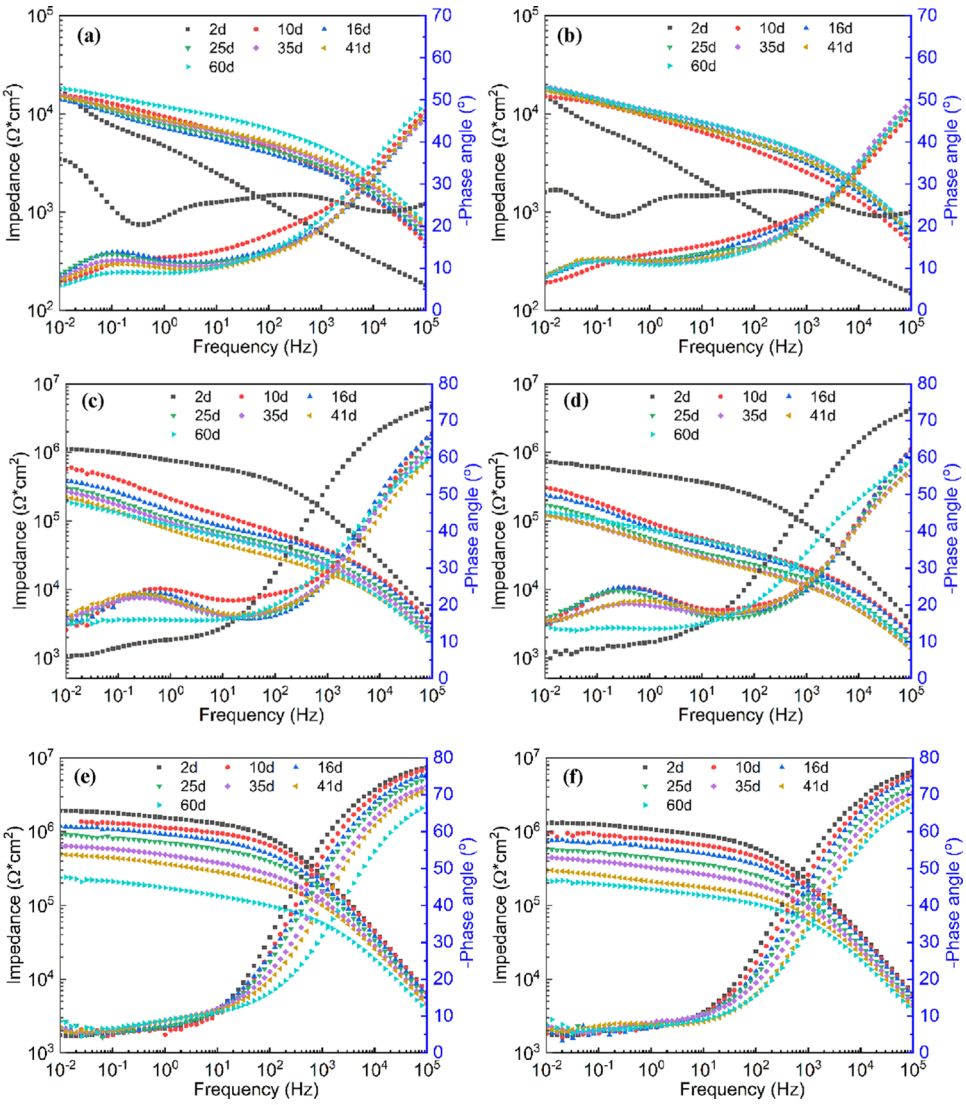

Figure 9. Bode plots of coatings immersed in 3.5 wt % NaCl solution up to 60 days. (a) 85ZRE; (b) 0.5ZF-85ZRE; (c) 75ZRE; (d) 0.5ZF-75ZRE; (e) 65ZRE; (f) 0.5ZF-65ZRE.

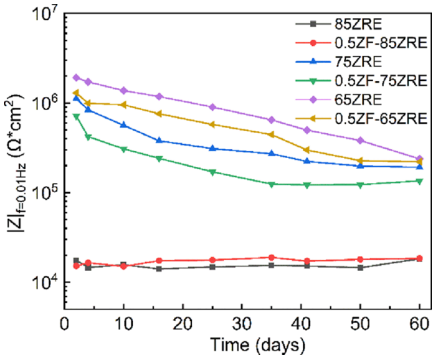

Figure 10. Impedance at low frequency ($|Z|_{f=0.01Hz}$) of coatings immersed in 3.5 wt % NaCl solution up to 60 days.

values of the 0.5ZF-75ZRE coating decreased during the first 41 days of immersion and then increased gradually to 135,500 Ω·cm^2 due to the improved barrier properties afforded by the zinc corrosion products. This is in good agreement with the OCP evolution. Further, the $|Z|_{f=0.01Hz}$ values of both 65ZRE and 0.5ZF-65ZRE coatings decreased continuously during the entire test period, implying a continuous penetration of the electrolyte. After 13 days of immersion, a few blisters and red rust spots were visually observed on the surface of 65ZRE and 0.5ZF-65ZRE coatings, which implies that both coatings had a low resistance to blistering and poor barrier property. The coatings lost their protectiveness to the steel substrate in a short time during immersion in 3.5 wt % NaCl solution. This agrees well with the study conducted by Shreepathi et al.,[37] where they found that ZRE coatings containing 60−70 wt % zinc provide neither good barrier protection nor effective cathodic protection to steel substrates.

The EIS results were further fitted using equivalent electrical circuits for interpreting the barrier property and the electrochemical reaction process. Figure 11 shows the equivalent circuit used for all coatings in this study. The equivalent circuit parameters obtained after EIS fitting are shown in Table S1 in Supporting Information, where R_s corresponds to the electrolyte resistance and R_c and CPE_c are related to the resistance and capacitance of the coating. R_{ct} and CPE_{dl} represent the charge transfer resistance and electrical double-layer capacitance associated with electrochemical reaction processes. Constant phase element (CPE) instead of capacitance was

https://doi.org/10.1021/acsomega.2c03738
ACS Omega 2023, 8, 1912−1922

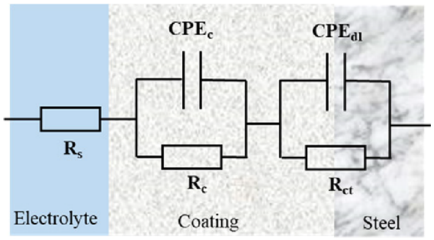

Figure 11. Equivalent electrical circuit used to fit the impedance spectra.

used due to the heterogeneity caused by surface roughness and dispersion effect of pigments, and it was calculated using the expression reported by Hsu and Mansfeld.[38]

Figure 12 shows the variations of coating resistance, coating CPE, charge transfer resistance, and double-layer CPE over immersion time. Coatings containing the same content of zinc dust exhibited a similar trend with regard to the evolution of R_c, CPE$_c$, R_{ct}, and CPE$_{dl}$ values despite the addition of zinc fibers. Further, the 0.5ZF-85ZRE coating show very similar R_c, CPE$_c$, R_{ct}, and CPE$_{dl}$ values to those of the 85ZRE coating, because the addition of zinc fibers had little influence on the coating porosity and electrical conductivity. During the entire test period, both 85ZRE and 0.5ZF-85ZRE coatings exhibited lower R_{ct} values accompanied by higher CPE$_{dl}$ values as compared to other coatings because of larger amounts of active zinc particles. However, they also displayed significantly lower R_c values and higher CPE$_c$ values because of a higher porosity of the coatings. The R_c value of both coatings exhibited a quick drop in the first 4 days, suggesting the electrolyte diffusion and activation of zinc particles, which agrees well with the OCP results. Later, the R_c value increased gradually, because the micropores within the coating were sealed by the formed corrosion products.

In contrast, coatings with 65 wt % zinc dust show a continuous decrease of R_c values accompanied by slightly increased CPE$_c$ values because of a continuous penetration of corrosive media. The R_c values of the 0.5ZF-65ZRE coating tend to be higher than the coating without zinc fibers during the late stage of immersion, which indicates that an better barrier protection was provided by a larger quantity of corrosion product precipitates at the coating/steel interface.

Among all coatings, the addition of zinc fibers showed a greatest effect on the electrochemical properties of the coating with 75 wt % zinc dust that is close to the electronic percolation threshold, and the addition of zinc fibers significantly improved the electrical conductivity. The R_c values declined rapidly during the first 10 days followed by a gradual decrease until 41 days, and showed a trend of increase during the remaining test time. Further, the 0.5ZF-75ZRE coating exhibited slightly higher R_c values during the late stage of immersion test, which implies that a larger amount of zinc corrosion products were formed (as also observed in Figure 6) because of more active zinc particles due to the presence of zinc fibers. This is consistent with the lower R_{ct} values.

3.5. Discussion of Anticorrosive Mechanisms of Coatings. According to previous studies,[2,39,40] the ZRE coating protects steel based on an initial cathodic protection of active zinc particles (i.e., zinc particles in direct electrical contact with steel or through other zinc particles) and a subsequent barrier protection enhanced by the formed corrosion products filling up micropores within the coating and/or precipitating on exposed steel in case of damage to the

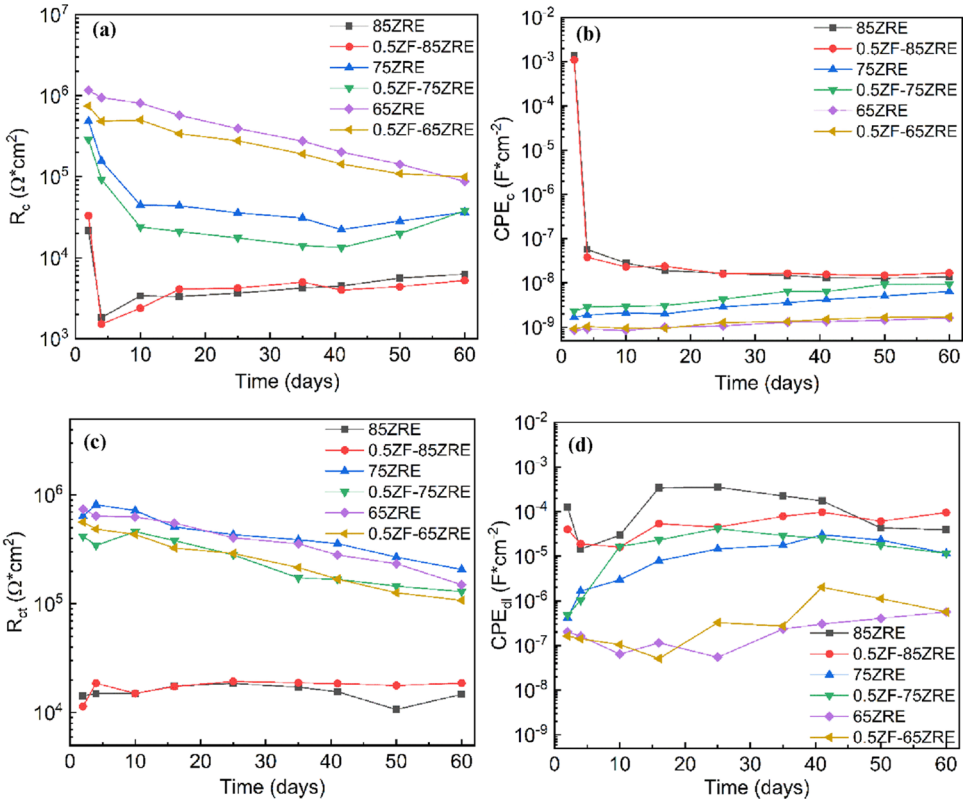

Figure 12. Variations of (a) coating resistance, (b) coating CPE, (c) charge transfer resistance, and (d) double-layer CPE over time.

https://doi.org/10.1021/acsomega.2c03738
ACS Omega 2023, 8, 1912−1922

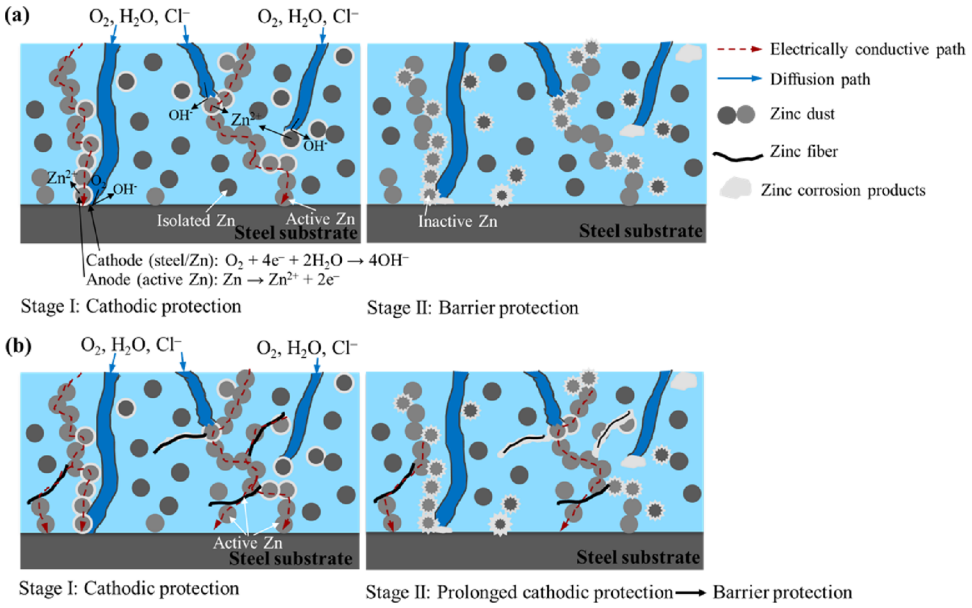

Figure 13. Illustration of anticorrosive mechanism for the ZRE coating (75 wt % zinc dust) (a) without and (b) with the addition of zinc fibers (note: this is an illustrative figure that does not present the actual fiber/particle ratio).

coating system. As shown in Figure 13a, at early stage, when zinc and steel are in contact within corrosive species (e.g., water, oxygen, and chloride ion) at defective/damaged areas of the coating, the surrounding zinc particles are activated (with a rapid drop of OCP), forming a galvanic cell with the exposed steel. The active zinc particles serve as an anode and sacrificially corrode to protect the steel substrate, which becomes a cathode. This cathodic protection is effective as long as there are sufficient active zinc particles, i.e., good electrical conductivity is persevered with OCP remaining below the cathodic protection limit. The galvanic action between zinc particles and the substrate results in the formation of zinc corrosion products, which tend to seal the pores/cracks. As the nonconductive corrosion products build up, conductive zinc particles are disconnected from each other and from steel and, consequently, cathodic protection is decayed. Subsequently, an enhanced barrier effect is provided by zinc corrosion products when OCP is above the cathodic protection limit.

Therefore, the cathodic protection of the ZRE coating is highly dependent on the zinc content because of the electronic percolation threshold. In this study, the results from the salt spray test, physiochemical characterization, and electrochemical tests show that coatings with 85 wt % zinc dust (85ZRE and 0.5ZF-85ZRE coatings) provided a superior cathodic protection, while coating containing 65 wt % zinc dust could not provide cathodic protection even with the addition of zinc fibers. In contrast, the 75ZRE coating showed a very short cathodic protection period, whereas the addition of 0.5 wt % zinc fibers significantly increased the cathodic protective activity of the coating. As shown in Figure 13b, initially, the presence of zinc fibers serves as a "bridge" to connect more zinc particles to the conductive percolation paths, increasing the amount of useful zinc particles. Over time, either spherical zinc dust particles or zinc fibers with a high specific surface area corrode, forming nonconductive zinc corrosion products. Compared to the 75ZRE coating, more electrical conductive percolation paths remain in the coating after the same exposure time. Consequently, the cathodic protection time is significantly prolonged for the 0.5ZF-75ZRE coating.

4. CONCLUSIONS

In this study, ZRE coatings containing various levels (65, 75, and 85 wt %) of zinc dust were prepared with and without the addition of 0.5 wt % zinc fibers, and the effect of zinc fibers on the corrosion protection performance of coatings was studied. The salt spray test results show that the role of zinc fibers in improving coating performance depends on the zinc dust content in the coating. The addition of 0.5 wt % zinc fibers showed a remarkably enhanced anticorrosion performance of the coating containing 75 wt % zinc dust, whereas no significant difference was observed for the coatings containing 65 and 85 wt % zinc dust. The results from SEM analysis and OCP and EIS measurements indicate that ZRE coatings containing 65 wt % zinc dust, even with the addition of zinc fibers, provided short-term barrier protection from the epoxy matrix, and the addition of zinc fibers further decreases the barrier effect because of the increased porosity. Coatings containing 85 wt % zinc dust exhibited superior cathodic protection, while the addition of zinc fibers did not show any remarkable influence on the coating properties. Coatings with 75 wt % zinc dust showed a mixed mechanism of cathodic and barrier protection, and the addition of 0.5 wt % zinc fibers reduced the impedance values but enhanced the cathodic protection significantly.

■ ASSOCIATED CONTENT

Supporting Information

The Supporting Information is available free of charge at https://pubs.acs.org/doi/10.1021/acsomega.2c03738.

SEM micrographs of zinc dust and zinc fiber, particle size distribution of zinc dust, replicate result of the salt spray test of different coatings, EDS mapping of coatings after 30 days salt spray test, replicate result of OCP measurements of different coatings, and EIS fitting data

https://doi.org/10.1021/acsomega.2c03738
ACS Omega 2023, 8, 1912−1922

with an equivalent circuit R(QR)(QR) for coatings immersed in 3.5 wt % NaCl solution (PDF)

AUTHOR INFORMATION

Corresponding Author

Hao Wu − *CHEC Research Center, Department of Chemical and Biochemical Engineering, Technical University of Denmark, 2800 Kgs. Lyngby, Denmark;* orcid.org/0000-0003-0462-2491; Email: haw@kt.dtu.dk

Authors

Chunping Qi − *The Hempel Foundation Coatings Science and Technology Centre (CoaST), Department of Chemical and Biochemical Engineering, Technical University of Denmark, 2800 Kgs. Lyngby, Denmark;* orcid.org/0000-0002-9098-1425

Claus Erik Weinell − *The Hempel Foundation Coatings Science and Technology Centre (CoaST), Department of Chemical and Biochemical Engineering, Technical University of Denmark, 2800 Kgs. Lyngby, Denmark*

Kim Dam-Johansen − *The Hempel Foundation Coatings Science and Technology Centre (CoaST), Department of Chemical and Biochemical Engineering and CHEC Research Center, Department of Chemical and Biochemical Engineering, Technical University of Denmark, 2800 Kgs. Lyngby, Denmark*

Complete contact information is available at: https://pubs.acs.org/10.1021/acsomega.2c03738

Notes

The authors declare no competing financial interest.

ACKNOWLEDGMENTS

The work is performed as part of the CoaST (The Hempel Foundation Coatings Science and Technology Centre). Financial support is obtained from the Hempel Foundation and the China Scholarship Council. A special thanks to Alicia Gutierrez Garcia for her assistance in formulations and discussions.

REFERENCES

(1) Cao, X.; Huang, F.; Huang, C.; Liu, J.; Cheng, Y. F. Preparation of Graphene Nanoplate Added Zinc-Rich Epoxy Coatings for Enhanced Sacrificial Anode-Based Corrosion Protection. *Corros. Sci.* **2019**, *159*, No. 108120.

(2) Tator, K. B. Zinc-Rich Coatings. In *ASM Handbook, Volume 5B, Protective Organic Coatings*, 2015; pp 213−220.

(3) Feliu, S. J.; Barajas, R.; Bastidas, J. M.; Morcillo, M.; Feliu, S. Study of Protection Mechanisms of Zinc-Rich Paints by Electrochemical Impedance Spectroscopy. In *Electrochemical Impedance: Analysis and Interpretation. ASTM STP 1188*; Sculty, J. R., Silverman, D. C., Kendig, M. W., Eds.; American Society for Testing and Materials, 1993; pp 438−449.

(4) Vilche, J. R.; Bucharsky, E. C.; Giúdice, C. A. Application of EIS and SEM to Evaluate the Influence of Pigment Shape and Content in ZRP Formulations on the Corrosion Prevention of Naval Steel. *Corros. Sci.* **2002**, *44*, 1287−1309.

(5) Weinell, C. E.; Rasmussen, S. N. Advancement in Zinc Rich Epoxy Primers for Corrosion Protection. In *CORROSION 2007*; OnePetro, 2007.

(6) Kalendová, A.; Veselý, D.; Kohl, M.; Stejskal, J. Anticorrosion Efficiency of Zinc-Filled Epoxy Coatings Containing Conducting Polymers and Pigments. *Prog. Org. Coat.* **2015**, *78*, 1−20.

(7) Park; Yun, T. H.; Kim, K. Y.; Song, Y. K.; Park, J. M. The Improvement of Anticorrosion Properties of Zinc-Rich Organic Coating by Incorporating Surface-Modified Zinc Particle. *Prog. Org. Coat.* **2012**, *74*, 25−35.

(8) Bastos, A. C.; Zheludkevich, M. L.; Ferreira, M. G. S. A SVET Investigation on the Modification of Zinc Dust Reactivity. *Prog. Org. Coat.* **2008**, *63*, 282−290.

(9) Arianpouya, N.; Shishesaz, M.; Arianpouya, M.; Nematollahi, M. Evaluation of Synergistic Effect of Nanozinc/nanoclay Additives on the Corrosion Performance of Zinc-Rich Polyurethane Nanocomposite Coatings Using Electrochemical Properties and Salt Spray Testing. *Surf. Coat. Technol.* **2013**, *216*, 199−206.

(10) Arman, S. Y.; Ramezanzadeh, B.; Farghadani, S.; Mehdipour, M.; Rajabi, A. Application of the Electrochemical Noise to Investigate the Corrosion Resistance of an Epoxy Zinc-Rich Coating Loaded with Lamellar Aluminum and Micaceous Iron Oxide Particles. *Corros. Sci.* **2013**, *77*, 118−127.

(11) Ehsanjoo, M.; Mohammadi, S.; Chaibakhsh, N. Long-Term Corrosion Resistance of Zinc-Rich Paint Using Functionalised Multi-Layer Graphene-Tripolyphosphate: In Situ Creation of Zinc Phosphate as Corrosion Inhibitor. *Corros. Eng., Sci. Technol.* **2019**, *54*, 698−714.

(12) Anandhi, A.; Palraj, S.; Subramanian, G.; Selvaraj, M. Corrosion Resistance and Improved Adhesion Properties of Propargyl Alcohol Impregnated Mesoporous Titanium Dioxide Built-in Epoxy Zinc Rich Primer. *Prog. Org. Coat.* **2016**, *97*, 10−18.

(13) Kowalczyk, K.; Spychaj, T. Zinc-Free Varnishes and Zinc-Rich Paints Modified with Ionic Liquids. *Corros. Sci.* **2014**, *78*, 111−120.

(14) Schaefer, K.; Miszczyk, A. Improvement of Electrochemical Action of Zinc-Rich Paints by Addition of Nanoparticulate Zinc. *Corros. Sci.* **2013**, *66*, 380−391.

(15) Jalili, M.; Rostami, M.; Ramezanzadeh, B. An Investigation of the Electrochemical Action of the Epoxy Zinc-Rich Coatings Containing Surface Modified Aluminum Nanoparticle. *Appl. Surf. Sci.* **2015**, *328*, 95−108.

(16) Armelin, E.; Martí, M.; Liesa, F.; Iribarren, J. I.; Alemán, C. Partial Replacement of Metallic Zinc Dust in Heavy Duty Protective Coatings by Conducting Polymer. *Prog. Org. Coat.* **2010**, *69*, 26−30.

(17) Akbarinezhad, E. Electrochemical Evaluations of Zinc-Rich Epoxy Primers Modified with Polyaniline and Exfoliated Polyaniline Graphite Nanocomposite. *Corros. Eng., Sci. Technol.* **2019**, *54*, 389−401.

(18) Akbarinezhad, E.; Ebrahimi, M.; Sharif, F.; Ghanbarzadeh, A. Evaluating Protection Performance of Zinc Rich Epoxy Paints Modified with Polyaniline and Polyaniline-Clay Nanocomposite. *Prog. Org. Coat.* **2014**, *77*, 1299−1308.

(19) Feliu, S.; Bastidas, J. M.; Morcillo, M.; Feliu, S. Effect of the Di-Iron Phosphide Conductive Extender on the Protective Mechanisms of Zinc-Rich Coatings. *J. Coat. Technol.* **1991**, 67−72.

(20) Qi, C.; Dam-Johansen, K.; Weinell, C. E.; Bi, H.; Wu, H. Enhanced Anticorrosion Performance of Zinc Rich Epoxy Coatings Modified with Stainless Steel Flakes. *Prog. Org. Coat.* **2021**, *163*, No. 106616.

(21) Li, Z.; Ravenni, G.; Bi, H.; Erik, C.; Ulusoy, B.; Zhang, Y.; Dam-johansen, K. Effects of Biochar Nanoparticles on Anticorrosive Performance of Zinc-Rich Epoxy Coatings. *Prog. Org. Coat.* **2021**, *158*, No. 106351.

(22) Gergely, A.; Pászti, Z.; Mihály, J.; Drotár, E.; Török, T. Galvanic Function of Zinc-Rich Coatings Facilitated by Percolating Structure of the Carbon Nanotubes. Part II: Protection Properties and Mechanism of the Hybrid Coatings. *Prog. Org. Coat.* **2014**, *77*, 412−424.

(23) Wang, D.; Sikora, E.; Shaw, B. A Comparison of the Corrosion Response of Zinc-Rich Coatings with and without Presence of Carbon Nanotubes under Erosion and Corrosion Conditions. *Corrosion* **2018**, *74*, 1203−1213.

(24) Teng, S.; Gao, Y.; Cao, F.; Kong, D.; Zheng, X.; Ma, X.; Zhi, L. Zinc-Reduced Graphene Oxide for Enhanced Corrosion Protection of Zinc-Rich Epoxy Coatings. *Prog. Org. Coat.* **2018**, *123*, 185−189.

(25) Wang, X.; Lv, J.; Ding, R.; Gui, T.; Sun, M. L. Application of EIS and Transmission Line Model to Study the Effect of Arrangement of Graphene on Electromagnetic Shielding and Cathodic Protection Performance of Zinc-Rich Waterborne Epoxy Coatings. *Int. J. Electrochem. Sci.* **2020**, *15*, 4089−4101.
(26) Giudice, C. Reinforcement Fibers in Zinc-Rich Nano Lithium Silicate Anticorrosive Coatings. In *Corrosion Resistance*; IntechOpen, 2012; pp 157−174.
(27) Ge, T.; Zhao, W.; Wu, X.; Lan, X.; Zhang, Y.; Qiang, Y.; He, Y. Incorporation of Electroconductive Carbon Fibers to Achieve Enhanced Anti-Corrosion Performance of Zinc Rich Coatings. *J. Colloid Interface Sci.* **2020**, *567*, 113−125.
(28) Eremiáš, B.; Mindoš, L.; Turek, L.; Hochmannova, L. The Application of ENA and Physico-Mechanical Tests for Evaluation of the Protective Performance of ZRP Modified by Combination of Zn Dust with Carbon Type Fillers. In *EUROCORR 2017 in combination with the 20th International Corrosion Congress and Process Safety Congress 2017*, 2017.
(29) BRITISH STANDARD ISO 9227. *Corrosion Tests in Artificial atmospheres—Salt Spray Tests*, 2006.
(30) Mouanga, M.; Beręot, P.; Rauch, J. Y. Comparison of Corrosion Behaviour of Zinc in NaCl and in NaOH Solutions. Part I: Corrosion Layer Characterization. *Corros. Sci.* **2010**, *52*, 3984−3992.
(31) De la Fuente, D.; Castaño, J. G.; Morcillo, M. Long-Term Atmospheric Corrosion of Zinc. *Corros. Sci.* **2007**, *49*, 1420−1436.
(32) Xu, L.; Liu, F.; Han, E. H.; Ke, W. Corrosion Resistance and Mechanism of One-Component Organic Zn15Al-Rich Coating. *Prog. Org. Coat.* **2019**, *132*, 305−315.
(33) Knudsen, O. Ø.; Steinsmo, U.; Bjordal, M. Zinc-Rich Primers - Test Performance and Electrochemical Properties. *Prog. Org. Coat.* **2005**, *54*, 224−229.
(34) Hammouda, N.; Chadli, H.; Guillemot, G.; Belmokre, K. The Corrosion Protection Behaviour of Zinc Rich Epoxy Paint in 3% NaCl Solution. *Adv. Chem. Eng. Sci.* **2011**, *01*, 51−60.
(35) Cubides, Y.; Su, S. S.; Castaneda, H. Influence of Zinc Content and Chloride Concentration on the Corrosion Protection Performance of Zinc-Rich Epoxy Coatings Containing Carbon Nanotubes on Carbon Steel in Simulated Concrete Pore Environments. *Corrosion* **2016**, *72*, 1397−1423.
(36) Xing, C.; Wang, W.; Qu, S.; Tang, Y.; Zhao, X.; Zuo, Y. Degradation of Zinc-Rich Epoxy Coating in 35% NaCl Solution and Evolution of Its EIS Parameters. *J. Coat. Technol. Res.* **2021**, *18*, 843−860.
(37) Shreepathi, S.; Bajaj, P.; Mallik, B. P. Electrochemical Impedance Spectroscopy Investigations of Epoxy Zinc Rich Coatings: Role of Zn Content on Corrosion Protection Mechanism. *Electrochim. Acta* **2010**, *55*, 5129−5134.
(38) Hsu, C. H.; Mansfeld, F. Concernng the Conversion of the Constant Phase Element Parameter Y0 into a Capacitance. *Corrosion* **2001**, *57*, 747−748.
(39) Theiler, F. The Rust Preventing Mechanism of Zinc Dust Paints. *Corros. Sci.* **1974**, *14*, 405.
(40) Sørensen, P. A.; Kiil, S.; Dam-Johansen, K.; Weinell, C. E. Anticorrosive Coatings: A Review. *J. Coat. Technol. Res.* **2009**, *6*, 135−176.

https://doi.org/10.1021/acsomega.2c03738
ACS Omega 2023, 8, 1912−1922